

## Strong decay widths of $b\bar{b}$ states above threshold

Seiji Ono

*Institut für Theoretische Physik der Rheinisch-Westfälischen Technischen Hochschule Aachen, 51 Aachen, Federal Republic of Germany*

(Received 14 April 1980)

The quark-pair-creation model is used to compute strong decay widths of  $b\bar{b}$  states above threshold. The result is compared with the recent data from the Cornell Electron Storage Ring.

### I. INTRODUCTION

Experiments at Fermilab<sup>1</sup> and DESY<sup>2</sup> show resonance structures  $\Upsilon$  and  $\Upsilon'$  which are generally understood as  $b\bar{b}$  states.  $\Upsilon''$  and  $\Upsilon'''$  were found by recent experiments at Cornell.<sup>3-5</sup>  $\Upsilon'''$  seems to lie above the strong decay threshold.<sup>5</sup> This nicely confirms the original prediction of three narrow states below threshold.<sup>6</sup>

In the present paper we study strong decay widths of  $b\bar{b}$  states above threshold,  $\Upsilon^* \rightarrow B\bar{B}$ , etc. We use the quark-pair-creation model (QPCM),<sup>7</sup> which is an extension of models by Micu<sup>8</sup> and by Carlitz and Kislinger.<sup>9</sup> In order to compute the matrix element we must know the wave functions of the initial and final mesons.

In Sec. II we show potentials which are used to determine these wave functions. In Sec. III strong decay rates of  $c\bar{c}$  and  $b\bar{b}$  states are calculated. In Sec. IV comments and discussions are presented.

### II. POTENTIALS

We use two nonrelativistic potentials for quarkonia, which not only explain  $c\bar{c}$  and  $b\bar{b}$  spectra correctly but also the  $D$  meson, the  $F$  meson, and even the old light-meson spectra. These two potentials were applied in models II and III, respectively, in our previous paper.<sup>10</sup>

Model II was originally proposed in Ref. 11 but with slightly different parameters. It is defined as follows:

$$V(R) = V_0(R) + V_{\text{INT}}(R) \quad (\text{model II}), \quad (1)$$

where

$$V_0(R) = V_{\text{AF}} + aR, \quad (2)$$

$$V_{\text{AF}}(R) = -\frac{4}{3} \frac{\alpha_s(R)}{R}, \quad \alpha_s(R) = \frac{12\pi}{25} \frac{1}{2 \ln(\mu/R)},$$

$$\mu = (\Lambda e^{\gamma_0})^{-1}, \quad \gamma_0 = 0.5772, \quad \Lambda = 0.5 \text{ GeV}.$$

$$V_{\text{INT}}(R) = -be^{-R/c}. \quad (3)$$

For large  $R$  the scalar confining part  $aR$  dominates in this potential. In the central region the behavior is essentially determined by  $V_{\text{AF}}$  which arises from one-gluon exchange with the running

coupling constant  $\alpha_s$ .  $V_{\text{AF}}$  is set to be constant for  $R > \mu/\exp(1)$ .

Model III is obtained from model II by the following replacement:

$$V_0(R) \rightarrow V_0'(R) = \begin{cases} -\frac{4}{3} \frac{\alpha_s}{R} + d & \text{for } R < R_1, \\ aR & \text{for } R \geq R_1. \end{cases} \quad (4)$$

$$d = 0.506 \text{ GeV}, \quad \alpha_s = 0.31,$$

$$R_1 = 0.322 \text{ fm} \quad (\text{model III}).$$

Following Ref. 10 we set the remaining parameters

$$a = 0.787 \text{ GeV/fm},$$

$$\left. \begin{aligned} b &= 1.378 \text{ GeV} \\ c &= 1.20 \text{ GeV}^{-1} \end{aligned} \right\} \text{for model II}, \quad (5)$$

$$\left. \begin{aligned} b &= 0.956 \text{ GeV} \\ c &= 2.05 \text{ GeV}^{-1} \end{aligned} \right\} \text{for model III}.$$

The reason we use these potentials here is that they predict correct masses for  $D$  and  $F$  mesons. We hope that our models also give an adequate description for  $B$  mesons. A candidate for a  $B$  meson with mass 5.3 GeV is reported,<sup>12</sup> which is close to our prediction by both models II and III.

### III. STRONG DECAY RATES

Before we study the processes  $\Upsilon$  (excited)  $\rightarrow B\bar{B}$ , etc., we should make sure that our models can explain the puzzling decay rates  $\psi(4028) \rightarrow D\bar{D}$ ,  $D\bar{D}^* + D^*\bar{D}$ ,  $D^*\bar{D}^*$ , etc. Related calculations already exist in the literature.<sup>13-21</sup>

In the QPCM the decay width for the two-body strong decay between mesons ( $A \rightarrow BC$ ) is given by

$$\Gamma = 2\pi \frac{E_B E_C}{M_A} k_B \gamma^2 \sum |M|^2, \quad (6)$$

where  $\gamma$  is a constant which specifies the strength of the pair creation. The explicit form of  $M$  is shown in the Appendix. The matrix element contains the following spatial overlap integral of the quark wave functions:

$$I(|\vec{k}_B|) = \int d\vec{q} y_1^m(\vec{q} + \frac{1}{2}h_c \vec{k}_B) \psi_A(\vec{q} - \frac{1}{2}h_c \vec{k}_B) \psi_B^*(\vec{q}) \psi_C^*(\vec{q}), \quad (7)$$

where

$$h_q = \frac{2m_c}{m_c + m_q} \text{ and } h_c = \frac{2m_q}{m_c + m_q} \quad (m_q = m_u, m_d).$$

The nodes in the wave function of radially excited states strongly influence the Zweig-rule-allowed decay widths.<sup>21</sup> The Cornell group<sup>13, 20</sup> has remarked on this point for  $c\bar{c}$  decays. Using the nonrelativistic QPCM, Le Yaouanc *et al.*<sup>14</sup> have explicitly shown that the puzzling experimental branching ratio<sup>22</sup> of  $\psi(4028)$  ( $k_B$ <sup>3</sup> phase-space factor is removed)

$$D^0\bar{D}^0 : D^0\bar{D}^{*0} + \bar{D}^0D^{*0} : D^{*0}\bar{D}^{*0} \\ = 0.2 \pm 0.1 : 4.0 \pm 0.8 : 128 \pm 40 \quad (8)$$

can be explained if the overlap integral  $I(|\vec{k}_B|)$  has the first node at  $|\vec{k}_B| = 0.686$  GeV/c. They used the harmonic-oscillator wave function for  $\psi(4028)$  and for  $D$  with the same spring constant which corresponds to the rms radius for the 1S state  $R^2 = 5.2$  GeV<sup>-2</sup> and assumed (i)  $m_c = m_q$  and (ii)  $\psi(4028)$  is a pure 3S state.

In models II and III the quark masses  $m_q = 0.336$  and  $m_c = 1.90$  GeV are used.<sup>10</sup> Therefore, our value for  $h_c$  is much smaller than that used by Le Yaouanc *et al.* Since all parameters are fixed to adjust to the mass spectra in our models we have no free parameter. Therefore, the overlap integral  $I(|\vec{k}_B|)$  is uniquely determined. Assuming that  $\psi(4028)$  is a pure 3S state we get the first nodes at  $|\vec{k}_B| = 0.687$  GeV/c (0.715 GeV/c) for model II (III), which are very close to what we need. The behavior of  $I(|\vec{k}_B|)$  in both models II and III is found to be very close to that predicted by Le Yaouanc *et al.*<sup>14</sup> which gives the ratio of

Eq. (8) correctly. The strong decay rates are calculated in both models and the results are shown in Table I. The parameter  $\gamma$  is used to obtain the best fit to the decay widths of  $\psi(3772)$ ,  $\psi(4028)$ , and  $\psi(4414)$ . We find  $\gamma = 2.2$  for both models. The agreement with the data is reasonably good.

This agreement is very encouraging. In this calculation we omit decay processes which include the  $D_P$  ( $D$  meson in the  $P$  wave), e.g.,  $\psi(4414) \rightarrow D_P\bar{D}$ . We expect that the mass of  $D_P$  is around 2520 MeV and  $\psi(4414) \rightarrow D_P\bar{D}$ ,  $D_P\bar{D}_P$ , etc., will be kinematically forbidden if the spin-orbit coupling is not very large. If we add the decay width of  $\psi(4414) \rightarrow D_P\bar{D}$  to the total width, it is possible that the agreement with the data can become even better. Thus we conclude that our models II and III give a satisfactory description of decay widths of  $c\bar{c}$  states above threshold.

We now try to extend our calculation to the  $b\bar{b}$  states. The mass spectrum by the model II is compared with the data from the Cornell Electron Storage Ring (CESR)<sup>3-5</sup> in Fig. 1. The agreement with the data is excellent. Model III predicts too large mass splittings, i.e.,  $\Upsilon'' - \Upsilon = 918$  MeV and  $\Upsilon''' - \Upsilon = 1192$  MeV. Thus model II is favored.

We compute the strong decay rates by using only model II. The strong decay rates are plotted as a function of  $\Delta = (\text{excited } b\bar{b}) - (\text{sum of final meson mass})$  in Figs. 2 and 3.

The results depend very sensitively on  $\Delta$ . Since it is impossible to have very precise prediction of  $\Delta$ , the unambiguous determination of the decay width is difficult.

The predicted masses of the  $B$  meson in model II (III) are  $B = 5250$  (5251),  $B^* = 5295$  (5307),  $B_s = 5332$  (5317) and  $B_s^* = 5368$  (5385) (in MeV).  $m_b = 5.25$  (5.29) GeV is assumed for model II (III) to estimate the value of  $\Delta$  for each process. How-

TABLE I. Strong decay widths of charmonium states predicted by model II and model III.

	Model II (MeV)	Model III (MeV)	Experiment (MeV)	Reference
$\psi_{3772}(1D) \rightarrow D\bar{D}$	22.5	21.4	$23.5 \pm 5$	22
$\psi_{4028}(3S) \rightarrow D\bar{D}$	2.44	0.934		
$\rightarrow D^*\bar{D} + D\bar{D}^*$	29.9	40.6		
$\rightarrow D^*\bar{D}^*$	34.8	33.0		
Total	67.2	74.6	$52 \pm 10$	17
$\psi_{4414}(4S) \rightarrow D\bar{D}$	9.31	7.26		
$\rightarrow D^*\bar{D} + D\bar{D}^*$	10.0	4.30		
$\rightarrow D^*\bar{D}^*$	3.03	8.63		
$\rightarrow F\bar{F}$	0.76	1.17		
$\rightarrow F^*\bar{F} + F\bar{F}^*$	4.17	4.10		
$\rightarrow F^*\bar{F}^*$	0.145	0.001		
Total	28.5	27.5	$33 \pm 10$	23
			$66 \pm 15$	24

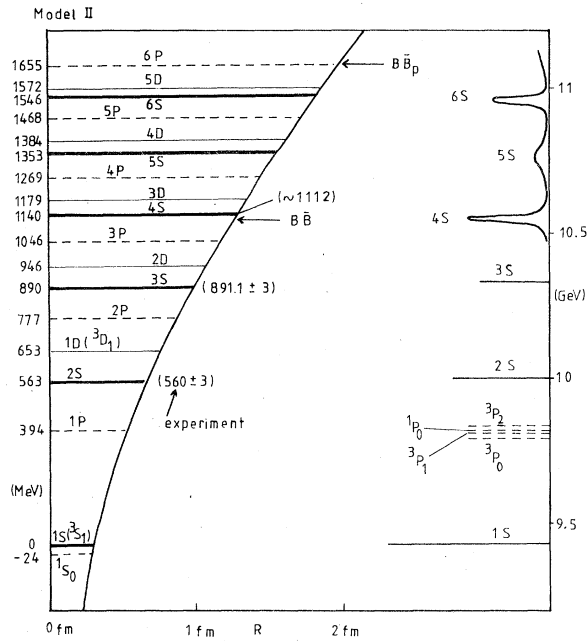


FIG. 1. The shape of the potential and the energy levels in model II.

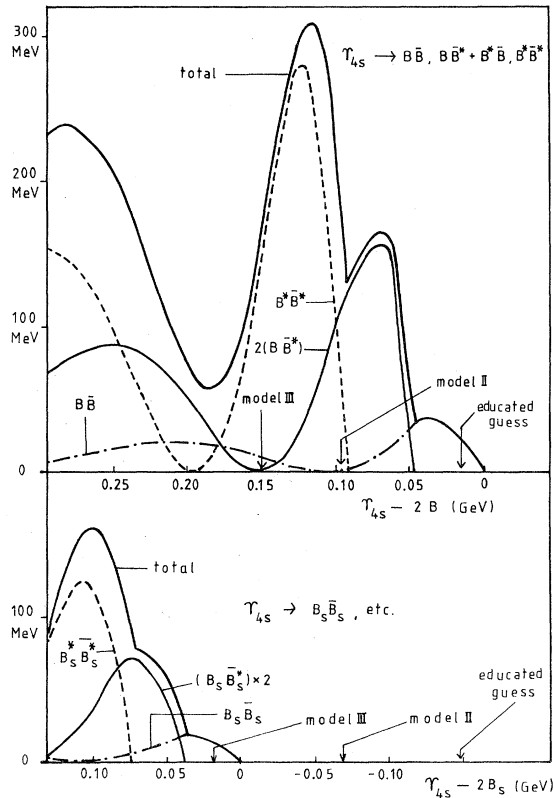


FIG. 2. Predicted widths of  $\Gamma_{4S}$  as a function of  $\Gamma_{4S} - 2B$  or  $\Gamma_{4S} - 2B_s$ . The predicted values for  $\Gamma_{4S} - 2B$  or  $\Gamma_{4S} - 2B_s$  are shown by arrows for models discussed in the text. An educated guess = ( $\Delta$  predicted by model II) = 80 MeV.

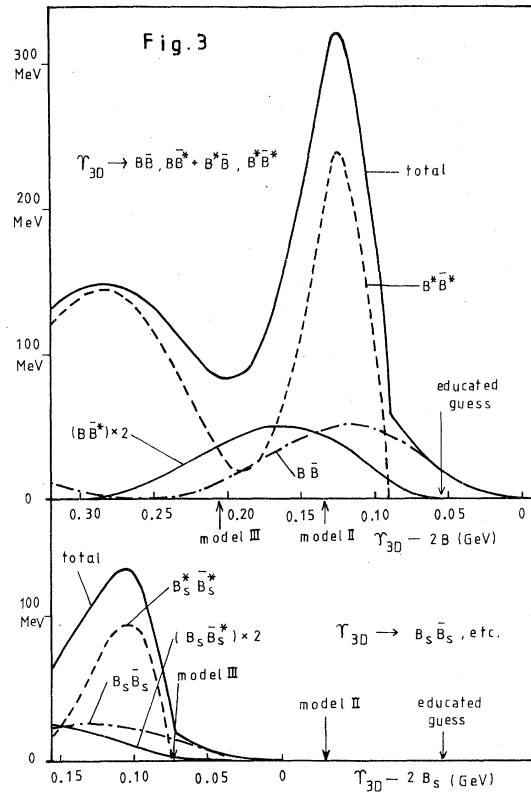


FIG. 3. Same as Fig. 2, but for  $\Gamma_{3D}$ .

ever, the following ambiguities remain in this determination. (i) We do not know the absolute mass of excited  $b\bar{b}$  states. DORIS data and CESR data are inconsistent with each other by around 20 MeV. (ii) Our estimation of the mass of the  $B$  meson will probably be correct within 1%, i.e.,  $\pm 50$  MeV. In some cases, a 10-MeV error in  $\Delta$  already causes too much error in the prediction of the strong decay rate.

On the other hand, the curve of the decay rate as a function of  $\Delta$  does not sensitively depend on models which we use, i.e., model II or model III. In Figs. 2 and 3 we plot decay widths as a function of  $\Delta$ , i.e.,  $\Gamma(\text{excited}) - 2B$  or  $\Gamma(\text{excited}) - 2B_s$  ( $B_s = b\bar{s}$ ) by using model II. The values of  $\Delta$  predicted by models II and III are shown by arrows in each figure.  $\gamma = 2.2$ , which is determined by the charmonium decay rates, is consistently used for all resonances.

#### IV. COMMENTS AND DISCUSSIONS

From Fig. 2 one can see that the total width of  $\Gamma_{4S}$  is more than 100 MeV if  $\Delta = 100\text{--}150$  MeV. The total width of  $\Gamma_{T''}$  obtained by CESR is  $\Gamma_{T''} = 19.8 \pm 5.5 \pm 5$  MeV (Ref. 5). This means that  $\Gamma''$  is just above the threshold and only the  $B\bar{B}$  decay

mode is allowed. Using this decay width one gets from Fig. 2,  $10 \leq \Upsilon''' - 2B \leq 50$  MeV. Assuming  $\Upsilon''' \sim 10.55$  GeV, the  $B$  meson becomes  $5.25$  GeV  $\leq B \leq 5.27$  GeV. If this argument is correct, the experimental evidence<sup>12</sup> of the meson at 5.300 GeV is slightly out of this range.

Our model prediction is around 5.25 GeV which is in this range. Anyway our model prediction of the value of  $\Delta$  will be somewhat overestimated (by about 80 MeV in model II). Let us assume that the value of  $\Delta$  is lower than our estimation of model II by 80 MeV for all  $\Upsilon$  located above threshold. From Figs. 2 and 3 and from direct calculations one obtains  $\Gamma(\Upsilon_{4S}) \sim 20$  MeV,  $\Gamma(\Upsilon_{5S}) \sim 80$  MeV,  $\Gamma(\Upsilon_{6S}) \sim 20$  MeV,  $\Gamma(\Upsilon_{3D}) \sim 20$  MeV, and  $\Gamma(\Upsilon_{4D}) \sim 80$  MeV.

All widths are below 100 MeV. This is just accidental because all of them avoided the large peak of  $\Upsilon^* \rightarrow B^* \bar{B}^*$ .  $\Gamma(\Upsilon_{6S})$  can be larger than the above value because the process  $\Upsilon_{6S} \rightarrow B \bar{B}_P$  ( $B_P$  is the  $B$  meson in the  $P$  state) is kinematically allowed. We expect the mass (center of gravity) of the  $B_P$  is around 5830 MeV.

Some comments are necessary here.

(i) Generally speaking, decay widths into  $B\bar{B}$ ,  $B\bar{B}^* + B^*\bar{B}$ ,  $B^*\bar{B}^*$  are larger than those into  $B_s\bar{B}_s$ ,  $B_s\bar{B}_s^* + B_s^*\bar{B}_s$ ,  $B_s^*\bar{B}_s^*$ . This result is caused by the difference of wave function between the  $B$  meson and the  $B_s$  meson. The wave function of the  $B_s$  meson in the momentum space has a larger width than that of the  $B$  meson because of the large reduced mass. On the other hand,  $b\bar{b}$  states above threshold have many nodes. Therefore, the integral  $I(|\vec{k}_B|)$  becomes smaller for the  $B_s$  meson than for the  $B$  meson due to the larger cancellations in the integral.

(ii) We are not very sure if  $\gamma$  is universal.  $\gamma$  for  $c\bar{c}$  may be different from that for  $b\bar{b}$ . In the string theory  $\gamma^2$  is probably proportional to the length of

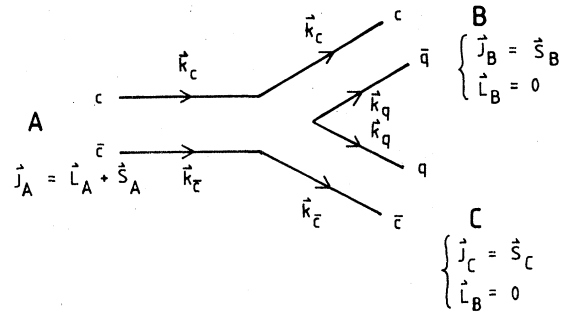


FIG. 4. Decay process  $A \rightarrow B + C$ .

the distance between the quark and the antiquark<sup>25</sup> (i.e., length of the string). However, this assumption does not change the value of  $\gamma$  very much. The running coupling constant  $\alpha_s$  for  $c\bar{c}$  is different from that for the  $b\bar{b}$ . Therefore,  $\gamma$  for  $c\bar{c}$  can be different from that for  $b\bar{b}$ .<sup>26</sup> It will be very difficult to calculate the  $M_q$  dependence of  $\gamma$  theoretically because we are assuming that many gluons are exchanged during the decay process.

(iii) In our model the peak of the curve of decay widths for  $\Upsilon_{4S}$  and  $\Upsilon_{3D}$  becomes very large. If the harmonic-oscillator potential is used the predicted widths become much smaller.<sup>27</sup> Since our potentials give correct scaling behavior of  $E_{2S} - E_{1S}$ , etc., as a function of  $m_q$  we believe that our potentials are more suitable for the  $b\bar{b}$  states.

#### ACKNOWLEDGMENTS

The author would like to thank O. Pene, A. Le Yaouanc, L. Oliver, and J. C. Raynal for much help and discussion. He wishes to thank P. Zerwas, H. Krasemann, M. Krammer, J. Jersak, and A. Martin for discussion. This research was supported by the Bundesministerium für Forschung und Technologie.

#### APPENDIX

The matrix element in Eq. (6) is expressed by (we use the notation of Le Yaouanc *et al.*)

$$M = \begin{bmatrix} i_1 & i_P & I_B \\ i_2 & i_P & I_C \\ I_A & 0 & I_A \end{bmatrix} \begin{bmatrix} S_1 & S_P & S_B \\ S_2 & S_P & S_C \\ S_A & 1 & S_T \end{bmatrix} \begin{bmatrix} L_A & S_A & J_A \\ 1 & 1 & 0 \\ L & S_T & J_A \end{bmatrix} \mathcal{L}(\pm),$$

where  $i$ ,  $S$ ,  $L$ , and  $J$  are isospin, spin, orbital angular momentum (see Fig. 4), and

$$\begin{bmatrix} j_{11} & j_{12} & j_{13} \\ j_{21} & j_{22} & j_{23} \\ j_{31} & j_{32} & j_{33} \end{bmatrix} \equiv [(2j_{13}+1)(2j_{23}+1)(2j_{31}+1)(2j_{32}+1)]^{1/2} \begin{Bmatrix} j_{11} & j_{12} & j_{13} \\ j_{21} & j_{22} & j_{23} \\ j_{31} & j_{32} & j_{33} \end{Bmatrix},$$

{ } is the  $9j$  symbol,

$$\begin{aligned}
\mathcal{L}(+) &\equiv \frac{(i)^{L_A}}{\sqrt{8}} \int_0^\infty r_A^2 dr_A u_{L_A}(r_A) \\
&\quad \times \int q^2 dq \tilde{u}_B(q) \tilde{u}_C(q) [q j_1(q r_A) j_{L_A+1}(\frac{1}{2} h_q k r_A) + \frac{1}{2} h_c k j_0(q r_A) j_{L_A}(\frac{1}{2} h_q k r_A)] \left[ \frac{3(L_A+1)}{2L_A+3} \right]^{1/2} \\
&\equiv \frac{(i)^{L_A}}{\sqrt{8}} \left[ \frac{3(L_A+1)}{2L_A+3} \right]^{1/2} I(+), \\
\mathcal{L}(-) &\equiv - \frac{(i)^{L_A}}{\sqrt{8}} \int_0^\infty r_A^2 dr_A u_{L_A}(r_A) \\
&\quad \times \int q^2 dq \tilde{u}_B(q) \tilde{u}_C(q) [-q j_1(q r_A) j_{L_A-1}(\frac{1}{2} h_q k r_A) + \frac{1}{2} h_c k j_0(q r_A) j_{L_A}(\frac{1}{2} h_q k r_A)] \left( \frac{3L_A}{2L_A-1} \right)^{1/2} \\
&\equiv - \frac{(i)^{L_A}}{\sqrt{8}} \left( \frac{3L_A}{2L_A-1} \right)^{1/2} I(-),
\end{aligned}$$

where

$$\vec{q} = \vec{k}_c \frac{m_q}{m_c + m_q} - \vec{k}_q \frac{m_c}{m_c + m_q}.$$

$\tilde{u}(q)$  is the S-state wave function in momentum space which is given by

$$\tilde{u}(q) \equiv \left( \frac{2}{\pi} \right)^{1/2} \int_0^\infty r^2 dr u_0(r) j_0(qr).$$

After the spin summation one gets

$$\begin{aligned}
\sum |M_{D\bar{D}}|^2 &= \frac{1}{96} I(+)^2, \\
\sum |M_{D\bar{D}^* D^* \bar{D}}|^2 &= \frac{1}{24} I(+)^2, \\
\sum |M_{D^* \bar{D}^*}|^2 &= \frac{7}{96} I(+)^2,
\end{aligned}$$

for  ${}^3S_1 \rightarrow D\bar{D}$ ,  $D\bar{D}^* + D^* \bar{D}$ ,  $D^* \bar{D}^*$ , and

$$\begin{aligned}
\sum |M_{D\bar{D}}|^2 &= \frac{1}{48} I(-)^2, \\
\sum |M_{D\bar{D}^* D^* \bar{D}}|^2 &= \frac{1}{48} I(-)^2, \\
\sum |M_{D^* \bar{D}^*}|^2 &= \frac{1}{120} I(-)^2 + \frac{3}{40} I(+)^2,
\end{aligned}$$

for  ${}^3D_1 \rightarrow D\bar{D}$ ,  $D\bar{D}^* + D^* \bar{D}$ ,  $D^* \bar{D}^*$ .

It can easily be checked that, from these equations, Eq. (3) in Ref. 15 and Eq. (7) in Ref. 14 can be derived by using the harmonic-oscillator wave function. We have done this check numerically and analytically.

- <sup>1</sup>S. W. Herb *et al.*, Phys. Rev. Lett. **39**, 252 (1977).  
<sup>2</sup>G. Flügge, in *Proceedings of 19th International Conference on High Energy Physics, Tokyo, 1978*, edited by S. Homma, M. Kawaguchi, and H. Miyazawa (Phys. Soc. of Japan, Tokyo, 1979), p. 793.  
<sup>3</sup>D. Andrews *et al.*, Phys. Rev. Lett. **44**, 1108 (1980).  
<sup>4</sup>T. Böhlinger *et al.*, Phys. Rev. Lett. **44**, 1111 (1980).  
<sup>5</sup>D. Andrews *et al.*, Phys. Rev. Lett. **45**, 219 (1980).  
<sup>6</sup>E. Eichten and K. Gottfried, Phys. Lett. **66B**, 286 (1980).  
<sup>7</sup>A. Le Yaouanc *et al.*, Phys. Rev. D **8**, 2223 (1973).  
<sup>8</sup>L. Micu, Nucl. Phys. **B10**, 521 (1969).  
<sup>9</sup>R. Carlitz and M. Kislinger, Phys. Rev. D **2**, 336 (1970).  
<sup>10</sup>S. Ono, Phys. Rev. D **20**, 2975 (1979).  
<sup>11</sup>H. Krasemann and S. Ono, Nucl. Phys. **B154**, 283 (1979).  
<sup>12</sup>B. Barate *et al.*, CERN Report No. CERN-EP-113, 1979 (unpublished).  
<sup>13</sup>E. Eichten lectured at the 1975 summer school on this subject [E. Eichten, in *Weak and Electromagnetic Interactions at High Energies*, Cargese, 1975, Part A, (Plenum, New York, 1976), pp. 305-328]. He dis-

- cussed in detail how the nodes of the  $c\bar{c}$  spatial wave function were manifest by a modulation of the decay amplitudes as a function of momentum, although he did not explicitly discuss the fact the  $D\bar{D}$ ,  $D\bar{D}^* + D^* \bar{D}$ , and  $D^* \bar{D}^*$  amplitudes would have different modulation patterns as a function of cms energy because of the different kinematics. This point was given explicitly in the paper by K. Lane and E. Eichten [Phys. Rev. Lett. **37**, 477 (1976)].  
<sup>14</sup>A. Le Yaouanc *et al.*, Phys. Lett. **71B**, 397 (1977).  
<sup>15</sup>A. Le Yaouanc *et al.*, Phys. Lett. **72B**, 57 (1977).  
<sup>16</sup>R. Barbieri, R. Kögerler, Z. Kunszt, and R. Gatto, Phys. Lett. **56B**, 477 (1975).  
<sup>17</sup>M. Chaichan and R. Kögerler, Phys. Lett. **80B**, 105 (1978).  
<sup>18</sup>A. Bradley and D. Robson, Manchester report, 1979 (unpublished).  
<sup>19</sup>A. Arneodo *et al.*, Z. Phys. C **3**, 37 (1979).  
<sup>20</sup>E. Eichten *et al.*, Phys. Rev. D **17**, 3090 (1978).  
<sup>21</sup>M. Böhm, H. Joos, and M. Krammer, Nucl. Phys. **B69**, 349 (1974).

<sup>22</sup>G. S. Abrams *et al.*, Phys. Rev. D 21, 2716 (1980).

<sup>23</sup>J. Siegrist *et al.*, Phys. Rev. Lett. 36, 700 (1976).

<sup>24</sup>R. Brandelik *et al.*, Phys. Lett. 76B, 361 (1978).

<sup>25</sup>J. Jersak, private communication.

<sup>26</sup>A. Martin, private communication.

<sup>27</sup>O. Pene, private communication.